Which one performs better for targeted lung cancer combination therapy: pre- or post-bombesin-decorated nanostructured lipid carriers?

Jiahui Du & Ling Li

Published online: 11 Oct 2015.

Submit your article to this journal ⎘

View related articles ⎘

View Crossmark data ⎘

Drug Delivery

Taylor & Francis
Taylor & Francis Group

RESEARCH ARTICLE

Which one performs better for targeted lung cancer combination therapy: pre- or post-bombesin-decorated nanostructured lipid carriers?

Jiahui Du[1] and Ling Li[2]

[1]Department of Thoracic Surgery, Linyi People's Hospital, Linyi, China and [2]Department of Clinical Laboratory, Linyi Cancer Hospital, Linyi, China

Abstract

Purpose: The co-delivery of gene and drugs has the potential to treat cancer. The aim of this study was to compare post-bombesin decorated nanostructured lipid carriers (NLC) carrying both doxorubicin (DOX) and DNA with pre-bombesin decorated NLC for lung cancer therapy. *Methods*: Post-bombesin decorated NLC were prepared by two steps. First, DOX and DNA-loaded NLC (DOX-DNA-NLC) was prepared. Second, Bombesin-NH$_2$ (BN-NH$_2$) was added into DOX-DNA-NLC to react with stearic acid-polyethylene glycol-COOH (SA-PEG-COOH) loaded in NLC. Pre-bombesin decorated NLC were prepared by two steps. First, Bombesin (BN)-conjugated ligands were synthesized. Second, DOX and DNA were loaded into BN decorated NLC. Their average size, zeta potential, drug and gene loading were evaluated. NCl-H460 human non-small lung cancer cells (NCl-H460 cells) were used for the testing of *in vitro* transfection efficiency and *in vitro* cytotoxicity. *In vivo* transfection efficiency and anti-tumor effect of NLC were evaluated on mice bearing NCl-H460 cells model.
Results: Post-bombesin decorated NLC has a particle size of 128 nm, DOX encapsulation efficiency (EE) of 85% and DNA EE of 91%. Pre-bombesin decorated NLC has a particle size of 101 nm, DOX EE of 86% and DNA EE of 92%. Post-bombesin decorated NLC displayed more stable and remarkably higher transfection efficiency and better anti-tumor ability than pre-bombesin decorated NLC both *in vitro* and *in vivo*.
Conclusion: Post-bombesin decorated NLC could function as better carriers to improve the cell targeting and nuclear targeting ability. The resulting nanomedicine could be a promising active targeting drug/gene therapeutic system for lung cancer therapy.

Introduction

Lung cancer is the leading cause of cancer-related deaths worldwide (Han et al., 2014). Current therapies for lung cancer treatment include chemotherapy, radiotherapy, and surgery. Chemotherapy continues to play an important role in the treatment of lung cancer; however, multidrug resistance (MDR) and severe adverse effects on normal tissues are major causes for failures in cancer chemotherapy (Shao et al., 2015). Therefore, novel treatment strategies for lung cancer are urgently needed. Combination chemotherapy for anticancer treatment is a promising strategy to generate synergistic anticancer effects, reduce individual drug-related toxicity, suppress MDR through different mechanisms of action, and reduce the dose of each agent required (Wang et al., 2015).

Nanotechnology-based drug delivery systems (DDS) have triggered enthusiasm in potential application for cancer treatment recently, and more and more nanomedicine for cancer therapy has been joined in clinical phase (Wicki et al., 2015). Nanotechnology-based DDS (Yang et al., 2011), commonly used for cancer therapy, include liposomes (Yang et al., 2009), carbon nanotubes, polymer micelles (Ahn et al., 2015), and nanoparticles (Nahire et al., 2014). However, these nanocarriers have some drawbacks, in particular for the efficient delivery of chemotherapeutics. Nanostructured lipid carriers (NLC) have attracted academic and industrial attention in the last few years and have the potential to be the ideal lipid-based carrier for co-delivery of chemotherapeutic and gene drugs (Taratula et al., 2013). NLC, developed from solid lipid nanoparticles (SLN), are composed of solid lipid matrices and spatially incompatible liquid lipids (Yang et al., 2013). Because of advantages of different lipids and their unique structures, NLC show a great number of advantages including: higher loading capability for drugs; less drug stacking capacity; less inclination of gelation; controlled drug release; passive and active targeting and produced most effortlessly on large industrial scale (Abdelwahab et al., 2013; Shi et al., 2013). Therefore, we designed an active targeting NLC for co-delivery of doxorubicin (DOX) and DNA for lung cancer therapy.

Active targeting delivery of anticancer drugs to cancer cells and tissues is a promising field for its potential to spare

Address for correspondence: Ling Li, Department of Clinical Laboratory, Linyi Cancer Hospital, No. 6 Lingyuandong Street, Linyi, 276001, China. Email: lilinglyph@hotmail.com

unaffected cells and tissues to decrease toxicity and improve effect. In order to enhance targeting, a high-affinity ligand, which binds selectively to a receptor on the cancer cells, is attached to the surface of a nanocarrier (Zhang et al., 2008). A great number of ligands have been published to modify NLC, including small molecules such as folic acid (Khajavinia et al., 2012), or macromolecules such as transferrin (Negi et al., 2014), hyaluronic acid (Chen et al., 2012), peptides (Kasongo et al., 2011), proteins (Wicki et al., 2015), etc. Of which hyaluronic acid, transferrin and bombesin have been published as active targeting ligands to treat lung cancer. Bombesin (BN) receptors, known as gastrin-releasing peptide receptors, have been found to be overexpressed in cell lines derived from several human tumor types, such as lung cancer, pancreatic cancer, prostate cancer, breast cancer, colon cancer, ovarian cancer and so on (Akhtar et al., 2014). BN is a linear tetra decapeptide with the sequence EQRLGNQWAVGHLM, which possesses homology to G-protein regulation at the amidated C terminal sequence in the final seven amino acids (Barve et al., 2014). Therefore, bombesin is the ideal ligand to target lung tumor.

As to decoration, it could be classified into two different methods, pre-decoration and post-decoration. Pre-decoration nanocarriers could be prepared by delivery of drugs with decorated vectors, while post-decoration nanocarriers can be obtained by surface decoration after drug-loaded carriers were prepared (Jiang et al., 2012). Researches have been published and elaborated different advantages of the two decorated methods: for pre-decoration, advantages including more stable for decorated vehicles (Kolhatkar et al., 2007; Yu & Zhang, 2009); for post-decoration, advantages including more efficient modification and better targeting capability (Kolishetti et al., 2010; Shahin et al., 2013). Post-PEGylated lipoplexes could be more promising vehicles for gene delivery than pre-PEGylated lipoplexes in retinal pigment epithelium cells (Peeters et al., 2007). Post-decorated SLN displayed more efficient DNA expression in rat Kupffer cells both *in vitro* and *in vivo* than pre-decorated SLN (Jiang et al., 2012; Hadinoto et al., 2013).

Combination therapy for cancers by co-delivery of chemotherapy drugs and DNA is another hot topic for following reasons: synergistic anticancer effects, lower multi-drug resistance, etc. (Gandhi et al., 2014; Tsouris et al., 2014). The efficacy of DOX, encapsulated in PEGylated liposome (Caelyx/Doxil), has been demonstrated by a number of authoritative clinical studies from preclinical studies to phase II studies (Yang et al., 2011).

In this paper, a novel conjugated ligand, bombesin-polyethylene glycol-stearic acid (BN-PEG-SA) was synthesized, and BN-PEG-SA decorated NLC carried both DOX and DNA was investigated. pAcGFP1-N1 encodes a green fluorescent protein (GFP) from *Aequorea coerulescens* (excitation maximum = 475 nm; emission maximum = 505 nm) was used as the model DNA. We compared two strategies for decoration by the same ligand (BN-PEG-SA). The characteristics of two kinds of decorated vehicles were compared using *in vitro* and *in vivo* transfection efficiency in human lung cancer cell line and animal model.

Materials and methods

Materials

Glycerol monostearate (GMS) was purchased from Shanghai Chineway Pharmaceutical Tech. Co Ltd. (Shanghai, China). Doxorubicin hydrochloride (DOX·HCl), bombesin, stearic acid (SA), oleic acid, Tween® 80, triethylamine (TEA) and Roswell Park Memorial Institute (RPMI) 1640 medium were purchased from Sigma-Aldrich Co., Ltd (St Louis, MO). 1,2-dioleoyl-3-trimethylammonium-propane (DOTAP; chloride salt) was obtained from Xi'an ruixi Biological Technology Co., Ltd (Xi'an, Shaanxi, China). Injectable soya lecithin was obtained from Shanghai Taiwei Pharmaceutical Co, Ltd (Shanghai, China). NH_2-PEG_{4000}-COOH was purchased from Shanghai Yarebio Co., Ltd (Shanghai, China). pAcGFP1-N1 was provided by Takara (Dalian) Biomedical Inc. (Liaoning, China). Quant-iT™ PicoGreen® dsDNA quantitation reagent was obtained from Invitrogen by Life Technologies (Carlsbad, CA). All other reagents used were of the highest quality commercially available.

Cells and animals

NCl-H460 human non-small lung cancer cells (NCl-H460 cells) were obtained from the American type culture collection (Rockville, MD), and maintained in the RPMI 1640 medium supplemented with 10% fetal bovine serum, 2 mM L-glutamine, 100 μg/ml penicillin G, and 100 μg/ml streptomycin at 37 °C in 5% CO_2 atmosphere.

Male BALB/c nude mice (4–6 weeks old, 18–22 g weight) were purchased from the Shanghai Slack Laboratory Animal Co., Ltd. (Shanghai, China), maintained at 25 °C and 55% of humidity with free access to standard water and chow. All animal experiments complied with the Animal Management Rules of the Ministry of Health of the People's Republic of China.

### Synthesis of SA-PEG$_{4000}$-COOH (SA-PEG-COOH)

SA-PEG-COOH was synthesized by a two-step reaction. The synthesis scheme is depicted in Figure 1. SA (2 mmol) was dissolved in tetrahydrofuran (THF). Then, N-hydroxysuccinimide (NHS) and 1-ethyl-3-(3-dimethylaminopropyl)-carbodiimide (EDC) were added to react at room temperature for 3 h. NHS-SA was obtained via rotary evaporation method and purification by high-performance liquid chromatography (HPLC).

NHS-SA (2 mmol) and NH_2-PEG_{4000}-COOH (2 mmol) were dissolved in THF and reacted under stirring at room temperature for 6 h. Finally, SA-PEG-COOH was obtained via rotary evaporation method and purification by HPLC.

Synthesis of bombesin-PEG$_{4000}$-SA (BN-PEG-SA)

BN-PEG-SA was obtained by the covalent amide bond between SA-PEG-COOH and the N-terminal of bombesin (Figure 1). SA-PEG-COOH was dissolved in THF. N-hydroxysuccinimide (NHS) and 1-ethyl-3-(3-dimethylaminopropyl)-carbodiimide (EDC) were added to react at room temperature for 3 h. Then, BN solution (1 mg/ml) was added, mixed well and kept for further stirring of 6 h. Finally,

Figure 1. Schematic representation of the synthesis of BN-PEG-SA ligands.
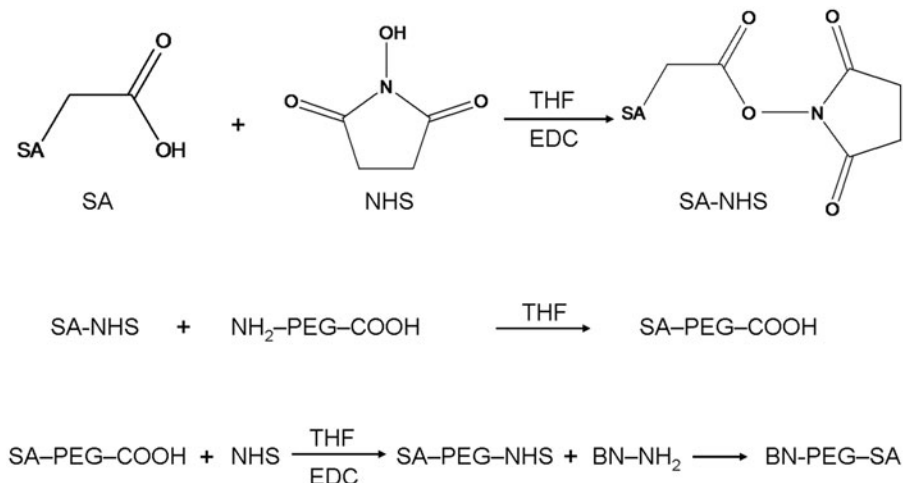
BN-PEG-SA was obtained via rotary evaporation method and purification by HPLC.

Preparation of DOX-loaded cationic NLC (DOX-NLC)

The doxorubicin base (DOX) was obtained by stirring with two equivalences of TEA in dimethyl sulfoxide (DMSO) overnight (Zhang et al., 2008). DOX-NLC was prepared by solvent diffusion method (Hejri et al., 2013; Luan et al., 2014). Briefly, the lipid dispersion was prepared by mixing GMS, oleic acid, soya lecithin, and PEG-SA (2:2:2:1, w/w). DOX was dissolved into ethanol (10 ml) and added to the lipid dispersion at 70–75 °C to obtain the organic phase. Meanwhile, the aqueous solution (15 ml) containing Tween 80 and DOTAP was heated at 70–75 °C. Then, the organic phase was immediately added into the aqueous solution under stirring at 1000 rpm at 70–75 °C for 20 min. The dispersion was cooled at room temperature and stirred until complete evaporation of the organic solvent to form NLC. The pellet was vortexed and re-suspended in distilled water, washed several times, filtered through a 0.8 μm membrane, and adjusted to pH 7.0 with sodium hydroxide. Blank NLC was prepared using the same method above, without the presence of DOX.

Preparation of post-bombesin decorated NLC

Post-bombesin decorated DOX-NLC

Post-bombesin decorated DOX-NLC (Post-BN-DOX-NLC) was prepared by utilizing the carboxylate group on the termini of SA-PEG on the DOX-NLC surface to attach the amine-terminated BN via EDC/NHS chemistry. In brief, 10 ml DOX-NLC were dispersed in 5 ml phosphate-buffered saline (PBS) and incubated with EDC and NHS (15 ml in total). Then, the dispersion was stirred gently for 3 h at room temperature. 500 μl, 1 ml, 2 ml, and 4 ml of BN solution (1 mg/ml) was added, mixed well and stirred for 6 h. Post-BN-DOX-NLC were collected after centrifugation at 10 000 rpm for 10 min and washed twice with distilled water. The conjugation efficiency was determined by measuring BN in supernatant by Bradford protein assay (Carlsson et al., 2011; Kulhari et al., 2014). The absorbance was measured at 595 nm using

UV-2550 UV/vis (ultraviolet/visible) spectrophotometer (Shimadzu, Japan).

Post-bombesin decorated DOX and DNA NLC

Post-bombesin decorated DOX and DNA NLC (Post-BN-DOX-DNA-NLC) was prepared by the electrostatic attraction method and based on Post-BN-DOX-NLC (Figure 2) (Peeters et al., 2007; Hadinoto et al., 2013). In brief, DNA (0.5 mg/ml) was added to an equal volume of Post-BN-DOX-NLC (5 mM DOTAP) by vortexing for 30 s. Incubation of the mixture for 30 min at room temperature facilitated formation of Post-BN-DOX-DNA-NLC. Post-BN-DOX-DNA-NLC was washed thrice with distilled water, lyophilized and stored at 2–8 °C. Undecorated DOX and DNA NLC (DOX-DNA-NLC) was prepared by the same method, using DOX-NLC instead of Post-BN-DOX-NLC.

Preparation of pre-bombesin decorated NLC

Pre-bombesin decorated DOX NLC

Pre-bombesin decorated DOX NLC (Pre-BN-DOX-NLC) was prepared by the same method mentioned in next section, except using BN-PEG-SA instead of SA-PEG-COOH.

Pre-bombesin decorated DOX and DNA NLC

Pre-bombesin decorated DOX and DNA NLC (Pre-BN-DOX-DNA-NLC) was prepared based on Pre-BN-DOX-NLC. DNA (0.5 mg/ml) was added to an equal volume of Pre-BN-DOX-NLC (5 mM DOTAP) by vortexing for 30 s (Figure 2). Incubation of the mixture for 30 min at room temperature facilitated the formation of Pre-BN-DOX-DNA-NLC. Pre-BN-DOX-DNA-NLC was washed thrice with distilled water, lyophilized and stored at 2–8 °C. Blank NLC was also prepared as described above without adding DOX and DNA.

Preparation of Lipo-DNA complexes

Lipo-DNA complexes were prepared as comparison for assessing the gene transfection efficacy of Pre-BN-DOX-DNA-NLC and Post-BN-DOX-DNA-NLC. The preparation method is the following (Kong et al., 2012): DNA and

Figure 2. Schematic diagrams showing the preparation of Pre-BN-DOX-DNA-NLC (A) and Post-BN-DOX-DNA-NLC (B).
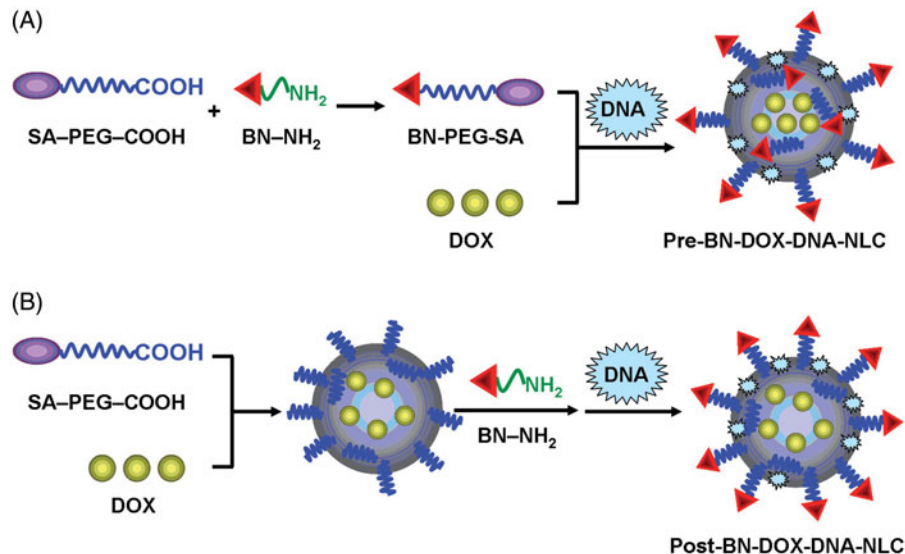
Lipofectamine 2000 (1:2, w/w) were mixed for 30 s using a vortex mixer. Then, DNA-loaded liposomes were obtained by incubating the mixture for 30 min.

Characterization of NLC formulations

The particle size (volume mean diameter), polydispersity index (PDI), and zeta potential of DOX-DNA-NLC, Post-BN-DOX-DNA-NLC, and Pre-BN-DOX-DNA-NLC were analyzed using photon correlation spectroscopy (PCS) with a Zetasizer 3000 (Malvern Instruments, Malvern, England).

The encapsulation efficiency (EE) and drug-loading content (DL) of DNA loaded into the Post-BN-DOX-DNA-NLC and Pre-BN-DOX-DNA-NLC was determined by the PicoGreen-fluorometry method (Hadinoto et al., 2013). Free DNA was isolated from Post-BN-DOX-DNA-NLC and Pre-BN-DOX-DNA-NLC by centrifugation at 10 000rpm at 4 °C for 30 min. Free DNA content in the supernatant was measured by a fluorescence spectrophotometer (HITACHI F2500, Tokyo, Japan).

To determine the EE and DL of DOX loaded into the Post-BN-DOX-NLC, Post-BN-DOX-DNA-NLC, Pre-BN-DOX-NLC, and Pre-BN-DOX-DNA-NLC, NLC dispersion was dispersed by pH adjustment. After the centrifugation, the NLC precipitate was harvested and the drug content in the supernatant was measured by HPLC (Agilent 1200 series, Santa Clara, CA). Chromatographic separations were achieved on a Inertsil® ODS-3 V column (250 mm × 4.6 mm) at 25 °C using a mobile phase of 50% (v/v) acetonitrile and 50% (v/v) phosphoric acid (0.01 M). Flow rate was kept at 1.0 ml/min and the detection was carried out at $\lambda = 254$ nm. Injection volume was 20 μl. The EE and DL of DNA and DOX was calculated by the following equations:

$$\mathrm{EE}(\%) = \frac{W_{\mathrm{total-drug}} - W_{\mathrm{free-drug}}}{W_{\mathrm{total-drug}}} \times 100 \quad (1)$$

$$\mathrm{DL}(\%) = \frac{W_{\mathrm{total-drug}} - W_{\mathrm{free-drug}}}{W_{\mathrm{total}}} \times 100 \quad (2)$$

$W_{\mathrm{total-drug}}$ is the weight of DNA or DOX added when preparing NLC; $W_{\mathrm{free-drug}}$ is the weight of the DNA or DOX measured in the supernatant; W_{total} is the weight of DNA, DOX, and NLC.

In vitro *drug release studies*

The amounts of DOX released from Post-BN-DOX-DNA-NLC, Pre-BN-DOX-DNA-NLC, DOX-DNA-NLC, and free DOX·HCl solution (free DOX) were measured by the dialysis method using PBS (pH 7.4, 50 ml) as dissolution medium. 5 ml of NLC mentioned above were placed in the dialysis bag respectively. The drug release tests were performed under horizontal shaking (SHELLAB1227-2 E, SHELLAB, Cornelius, OR) at 37 °C and 100 rpm. At predetermined time points, 1 ml of medium was collected and all residual medium outside the dialysis membrane was replaced with fresh PBS. The DOX concentrations were determined by the HPLC method mentioned above. The DNA concentrations were analyzed by the PicoGreen assay.

In vitro *cytotoxicity experiments*

In vitro cytotoxicity experiments of Post-BN-DOX-DNA-NLC, Pre-BN-DOX-DNA-NLC, DOX-DNA-NLC, free DOX, and blank NLC against NCl-H460 cells were performed by 3-(4,5-dimethylthiazol-2-yl)-2,5-diphenyltetrazolium bromide (MTT) assay (Mosmann, 1983). All concentrations were expressed in DOX equivalents. Briefly, NCl-H460 cells were seeded into a 48-well microplate at a density of 5000 cells per well. After 24 h, the culture medium was removed, and 0.9% saline (the control group), various concentrations of formulations (1, 2, 5, 10, 20 μM) were added and incubated for 48 h at 37 °C in 5% CO$_2$ atmosphere. Culture medium was used as the blank control group. Then, cell viability (CV) was determined by MTT assay. 20 μl of MTT solution (5 mg/ml in PBS) was added to each well and the cells were incubated for another 4 h at 37 °C in 5% CO$_2$ atmosphere. Then, the medium was removed carefully and 200 μl of DMSO was added to each well to dissolve the formazan crystals, and the

optical density (OD) of the obtained DMSO solution was measured at 570 nm by microplate reader (Model 680, Bio-Rad, Hercules, CA). CV was calculated as follows:

$$\mathrm{CV}(\%) = \frac{OD_{\text{sample}} - OD_{\text{blank}}}{OD_{\text{control}} - OD_{\text{blank}}} \times 100 \qquad (3)$$

The cytotoxicity was expressed as IC_{50}, which was defined as the concentration that caused 50% inhibition of CV and was calculated by the Logit method (Armutlu et al., 2008).

In vitro *transfection experiments*

For *in vitro* transfection, NCl-H460 cells were seeded into a 48-well microplate at a density of 1.5×10^5 cells per well. After 24 h, the culture medium (complete medium) was removed, and Post-BN-DOX-DNA-NLC, Pre-BN-DOX-DNA-NLC, DOX-DNA-NLC, Lipo-DNA, naked DNA solution, blank NLC were added and incubated for another 4 h at 37 °C in 5% CO_2 atmosphere. The medium containing the complexes in wells was refreshed with 1 ml of complete medium. Cells were incubated for another 72 h. At the end of the incubation, cells were washed once with PBS and detached with trypsin/ethylenediaminetetraacetic acid (EDTA). Then, cells were centrifuged and the supernatant was discarded. Finally, cells were resuspended with PBS and added into the flow cytometer to quantify transfection efficacy.

In vivo *gene transfection experiments*

Tumor-bearing mice were received an intravenous injection of Post-BN-DOX-DNA-NLC, Pre-BN-DOX-DNA-NLC, Lipo-DNA, naked DNA solution, or blank NLC (6 mice per group, 10 mg DNA per injection). After 3 d, mice were sacrificed and tumor tissues were removed and soaked with 75% ethanol for 3 s. Then, tumor tissues were washed with Hank's solution for three times, minced with a surgical scissor into pieces (about 1 mm^2), and washed with Hank's solution for another three times. 0.25% trypsin was then added at 37 °C during vibration every 5 min for 30 min to isolate cells. 5 ml of complete medium was added to stop digestion. The upper suspension was obtained by standing for 10 min, added to centrifuge tube, and centrifugation (4 °C, $1000 \times g$) for 5 min. The supernatant was discarded and 5 ml of Hank's solution was added. Cells were obtained by centrifugation and abandon of supernatant. Finally, cells were seeded into 24-well plates in the complete medium and observed using an inverted fluorescence microscope (Olympus ZX71; Olympus Corp, Tokyo, Japan). For quantitation, cells were washed with 1 ml of PBS (4 °C, 100 g, for 5 min) and were detached with trypsin/EDTA. The supernatant was discarded and resuspended with PBS and added into the flow cytometer to quantitate the amount of NCl-H460 cells which were successfully transfected.

In vivo *anti-tumor efficacy*

Male BALB/c nude mice were inoculating subcutaneously in the back with 100 μl NCl-H460 cells (10^6 cells) suspended in PBS (Ogawara et al., 2009). When the tumor volume reached about 100 mm^3, mice were divided into five groups (six mice

per group): (A), the control group, 0.9% sodium chloride solution; (B), free DOX (3 mg/kg); (C), DOX-DNA-NLC (3 mg/kg); (D), Pre-BN-DOX-DNA-NLC (3 mg/kg); and (E), Post-BN-DOX-DNA-NLC (3 mg/kg). The mice of each group were treated with the above five recipes by tail vein injection every week for six weeks. Tumor volume (V) and body weight (W) were measured every week. Tumor volume was calculated using the following equation:

$$V(\text{mm}^3) = \frac{L \times W^2}{2} \qquad (4)$$

L and W represent the largest diameter and the smallest diameter, respectively.

Tumor inhibition rate (TIR) was used to assess *in-vivo* antitumor efficacy. TIR was calculated using the following equation:

$$\mathrm{TIR}(\%) = \frac{W_{\text{control}} - W_{\text{sample}}}{W_{\text{control}}} \times 100 \qquad (5)$$

Statistical analysis

All studies were repeated three times and all measurements were carried out in triplicate. Results were reported as means $\pm$ SD (SD = standard deviation). Statistical significance was tested by two-tailed Student's *t*-test or one-way analysis of variance. Differences between experimental groups were considered significant when the *p* value was less than 0.05 ($p < 0.05$).

Results

Structure confirmation of SA-PEG-COOH and BN-PEG-SA

Structure confirmation of SA-PEG-COOH and BN-PEG-SA was performed by infrared (IR) spectroscopy and nuclear magnetic resonance spectroscopy (^{1}H NMR).

SA-PEG-COOH: IR ν/cm^{-1}: 3,239(–OH, –NH–); 3,116(–CO–O–); 2,966(–CH$_3$); 2,916(–CH$_2$–); 1,706(–OH), 1,623(–NH–CO–); 1,366(–CO–O–); 712(–NH–). ^{1}H NMR (DMSO-d$_6$, 300 MHz), δ (ppm): 0.92(t, –CH$_3$); 1.15–1.92(s, –CH$_2$); 2.26(s, –NH$_2$); 4.07(t, –CO–O–); 4.22(t, –CO–O–); 4.43(s, –NH–); 11.21(s, –OH). The peaks of –NH–CO–, –CO–O–, –OH, and –CH$_3$ peaks identified the structure of SA-PEG-COOH. The yield was around 80%.

BN-PEG-SA: IR ν/cm^{-1}: 3,430(–NH$_2$); 3,249(–NH–); 2,931(–CH$_2$–); 1635(–NH–CO–); 1,539(–C$_6$H$_5$); 1,282(–S–CH$_2$–); 768(–C$_6$H$_5$). ^{1}H NMR (DMSO-d$_6$, 300 MHz), δ (ppm): 1.26–2.23(s, –CH$_3$), 2.00(s, –NH$_2$), 2.09(s, –S–CH$_2$–), 2.40(s, –S–CH$_2$–), 7.08–7.26(m, –C$_6$H$_5$, Benzene ring of BN). The peaks of –NH–CO–, –CO–O–, –S–CH$_2$–, –NH$_2$, and –C$_6$H$_5$ peaks identified the structure of SA-PEG-COOH. The yield was around 70%.

Quantification of conjugation of BN to NLC surface

For Post-BN-DOX-DNA-NLC, BN was conjugated to the NLC surface by well-known EDC/NHS reaction. The conjugation was carried out in four different ligand/carrier ratios: 500 μl, 1 ml, 2 ml, and 4 ml of BN solution (1 mg/ml) was added and named Post-NLC1, Post-NLC2, Post-NLC3, Post-NLC4,

Table 1. Quantification of conjugation of BN to NLC surface.

Formulations	Particle size (nm)	Size distribution (PDI)	Zeta potential (mV)	Conjugation efficiency (%)	Conjugation ratio (μg/mg)
DOX-DNA-NLC	86.61 ± 2.35	0.096 ± 0.019	+8.6 ± 1.1	–	–
Post-NLC1	109.23 ± 3.28	0.123 ± 0.023	+16.8 ± 2.3	95.68 ± 1.46	8.0 ± 0.3
Post-NLC2	115.36 ± 3.51	0.147 ± 0.022	+21.4 ± 2.8	91.34 ± 2.97	15.2 ± 0.7
Post-NLC3	126.76 ± 2.69	0.102 ± 0.021	+28.8 ± 1.9	85.68 ± 2.52	28.6 ± 0.6
Post-NLC4	128.14 ± 4.15	0.184 ± 0.028	+29.1 ± 3.6	43.12 ± 3.09	28.7 ± 0.8

Table 2. Characterization of different NLC formulations.

Formulations	Particle size (nm)	Size distribution (PDI)	Zeta potential (mV)	DNA EE (%)	DOX EE (%)	DNA DL (%)	DOX DL (%)
Blank NLC	82.55 ± 2.19	0.097 ± 0.011	+21.5 ± 3.3	–	–	–	–
DOX-DNA-NLC	85.97 ± 2.28	0.112 ± 0.018	+8.7 ± 0.9	91.5 ± 2.6	86.7 ± 3.3	8.3 ± 1.5	2.3 ± 0.6
Post-BN-DOX-DNA-NLC	128.03 ± 2.31	0.165 ± 0.021	+28.4 ± 1.8	90.8 ± 2.3	85.3 ± 2.9	5.2 ± 0.9	1.4 ± 0.4
Pre-BN-DOX-DNA-NLC	101.36 ± 2.31	0.134 ± 0.020	+23.7 ± 2.5	91.7 ± 2.1	86.2 ± 3.1	5.7 ± 1.1	1.6 ± 0.3
Lipo-DNA complexes	178.64 ± 8.76	0.153 ± 0.032	+26.4 ± 2.1	90.2 ± 3.2	–	6.2 ± 1.2	–

respectively. The particle size, zeta potential, conjugation efficiency, the weight ratio of BN conjugated to per mg of NLC (conjugation ratio, W_{BN}/W_{NLC}, μg/mg) were measured and summarized in Table 1. As the BN ligands ratio increased, the particle size and zeta potential of Post-BN-DOX-DNA-NLC increased from Post-NLC1 to Post-NLC3. While from Post-NLC3 to Post-NLC4, no obviously change was found of the size and potential. The conjugation efficiency was slightly decreased with the growth in ligands concentration until Post-NLC3, but sharply declined from Post-NLC3 to Post-NLC4. Conversely, the conjugation weight ratio of BN conjugated to per mg of NLC was increased all the way to Post-NLC3, but no significant change was found between Post-NLC3 and Post-NLC4. These results demonstrated that the ligand/carrier ratio could be increased to 2 ml of BN solution versus 15 ml DOX-NLC (Post-NLC3), and then any further increase in BN ligands ratio could not bring about better decoration effect. So this ratio was determined and used for the following experiments of the post-bombesin decorated NLC.

To select the amount of BN in the pre-bombesin decorated NLC, we would like to make it the same (μg/mg of NLC) as the post-bombesin decorated ones. The amount of BN-PEG-SA was calculated according to the quantity of BN in the above mentioned Post-NLC3, and then applied for the preparation of Pre-BN-DOX-DNA-NLC.

Characterization of NLC formulations

The particle size, zeta potential, EE, and DL of all kinds of NLCs were analyzed and summarized in Table 2. The size of Post-BN-DOX-DNA-NLC was 128 nm, and Pre-BN-DOX-DNA-NLC was 101 nm. Decoration of BN increased the NLC size, larger than DOX-DNA-NLC (86 nm) and blank NLC (83 nm). The zeta potential of modified NLC was higher than unmodified NLC, this phenomenon could be explained by the positive charge of BN increased the particles' surface charge. The DNA EE and DOX EE of all the studied formulations was around 90% and 85%, respectively.
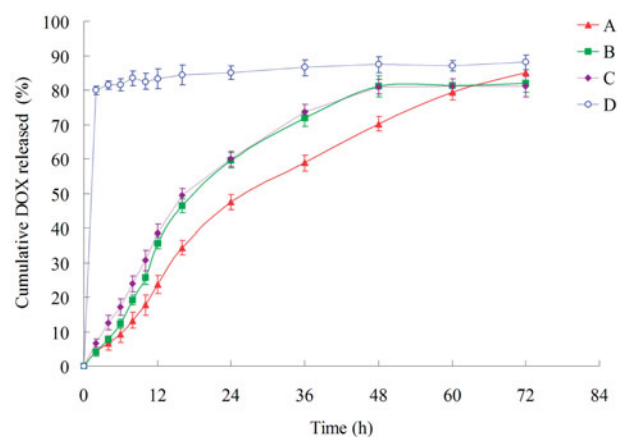

Figure 3. *In vitro* DOX release profile of Post-BN-DOX-DNA-NLC (A), Pre-BN-DOX-DNA-NLC (B), DOX-DNA-NLC (C), and Free DOX (D).

In vitro drug release

In vitro accumulated DOX release profiles and DNA release profiles of Post-BN-DOX-DNA-NLC, Pre-BN-DOX-DNA-NLC, DOX-DNA-NLC, and free DOX were calculated in Figures 3 and 4, respectively. The release of DOX from Post-BN-DOX-DNA-NLC was the slowest, reaching over 80% of DOX accumulation at 72 h. Release behavior of Pre-BN-DOX-DNA-NLC and DOX-DNA-NLC are similar, after 48 h of study, 81.2% and 80.9% of DOX released from the vectors, respectively. DOX released from free DOX solution was much faster than NLC formulations, achieved around 80% drug release at 2 h.

The DNA release of DOX-DNA-NLC was the fastest, followed by Pre-BN-DOX-DNA-NLC, and Post-BN-DOX-DNA-NLC was the most sustained-released. All the formulations reached about 85% of gene release at 72 h.

Cytotoxicity assays

Using the MTT method, the viability of NCl-H460 cells with different formulations was determined for
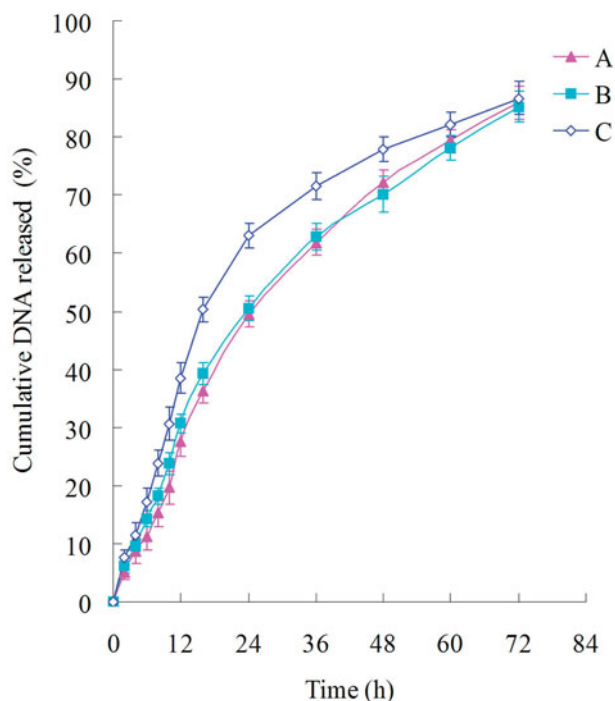
Figure 4. *In vitro* DNA release profile of Post-BN-DOX-DNA-NLC (A), Pre-BN-DOX-DNA-NLC (B), and DOX-DNA-NLC (C).
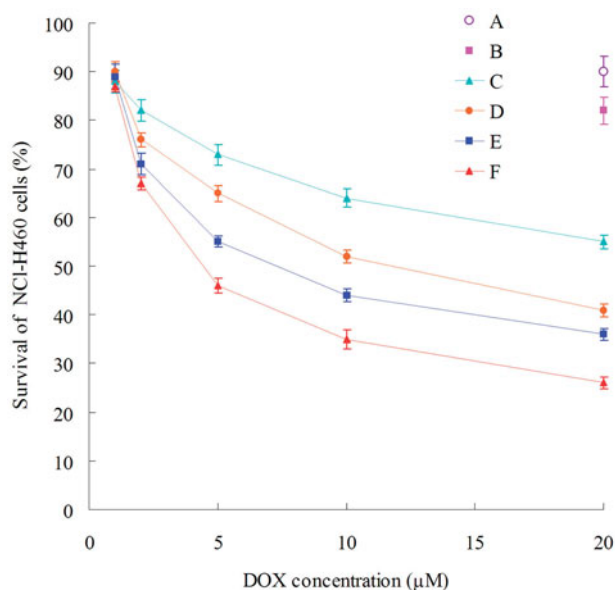

Figure 5. *In vitro* cytotoxicity of blank control (A), blank NLC (B), free DOX (C), DOX-DNA-NLC (D), Pre-BN-DOX-DNA-NLC (E), and Post-BN-DOX-DNA-NLC (F).

cytotoxicity investigation. As shown in the Figure 5, blank NLC showed low toxicity due to high CV (over 80%). Significantly inhibitory effects were observed in the DOX containing formulations at the concentration of 1–20 μM, and the toxicity conformed to a dose-dependent manner. The IC_{50} values of Post-BN-DOX-DNA-NLC, Pre-BN-DOX-DNA-NLC, DOX-DNA-NLC, and free DOX were 4.5, 8.1, 12.3, and 26.7 μM, respectively. The IC_{50} of Post-BN-DOX-DNA-NLC exhibited 2-fold dose advantage over Pre-BN-DOX-DNA-NLC, 3-fold of DOX-DNA-NLC, and 6-fold compared with free DOX in reducing viability of lung cancer cells,
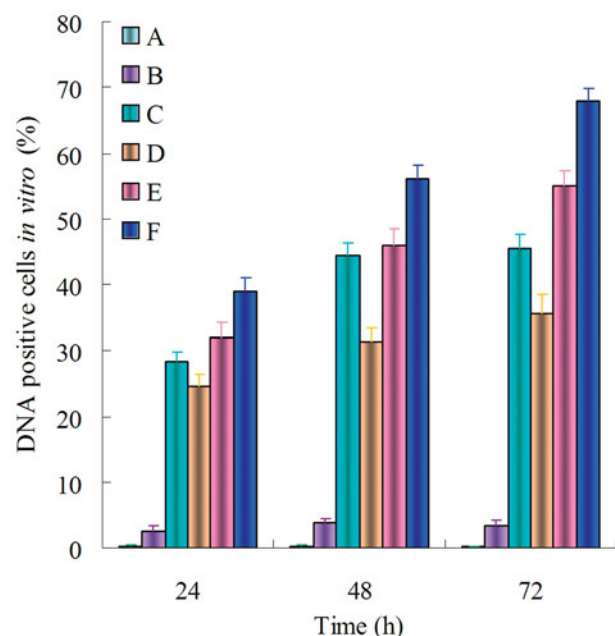

Figure 6. *In vitro* gene transfection of blank NLC (A), naked DNA solution (B), Lipo-DNA (C), DOX-DNA-NLC (D), Pre-BN-DOX-DNA-NLC (E), and Post-BN-DOX-DNA-NLC (F).

revealing the highest tumor cell toxicity. This property may lead to a better anti-tumor effect of the post-decorated NLC over their pre-modified counterparts.

In vitro and *in vivo* gene transfection

Figure 6 shows the percentage of cells transfected 24, 48, and 72 h after the addition of blank NLC, naked DNA solution, Lipo-DNA, DOX-DNA-NLC, Pre-BN-DOX-DNA-NLC, and Post-BN-DOX-DNA-NL *in vitro*. BN decorated NLC formulations induced a high transfection level than undecorated and Lipofectamine groups. The highest transfection level was reached by Post-BN-DOX-DNA-NLC at 72 h (67.9 ± 1.9%) transfection efficiency was significantly higher than other formulations ($p < 0.05$).

In vivo gene transfection studies of different formulas were carried out on BALB/c nude mice. The highest transfection activity (Figure 7) was obtained with Post-BN-DOX-DNA-NLC at 48 and 72 h. This transfection level was statistically higher than the Pre-BN-DOX-DNA-NLC, DOX-DNA-NLC and Lipo-DNA ($p < 0.05$). However, no significant differences were detected between Pre-BN-DOX-DNA-NLC and undecorated DOX-DNA-NLC at all the studied time points ($p > 0.05$).

In vivo anti-tumor activity

The formulations were injection every week, and the tumor size and body weight were then monitored every week at the time before injection. The results in Figure 8 showed that Post-BN-DOX-DNA-NLC had the highest efficacy in inhibiting the tumor growth than Pre-BN-DOX-DNA-NLC and other formulations ($p < 0.05$). The NLC formulas were more effective than free DOX solution. At the end of experiment, the TIR of lung cancer bearing mice treated with the Post-BN-DOX-DNA-NLC was 76%, which was about 1.5 times, 2.1 times, and 5.6 times higher than that treated with
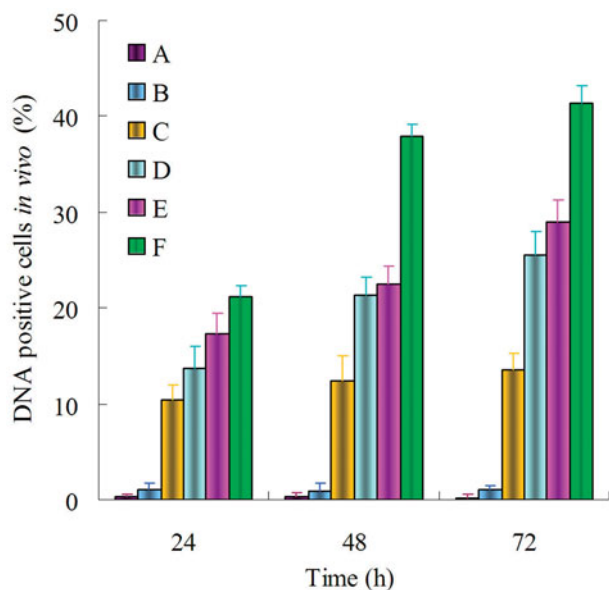
Figure 7. *In vivo* gene transfection of blank NLC (A), naked DNA solution (B), Lipo-DNA (C), DOX-DNA-NLC (D), Pre-BN-DOX-DNA-NLC (E), and Post-BN-DOX-DNA-NLC (F).
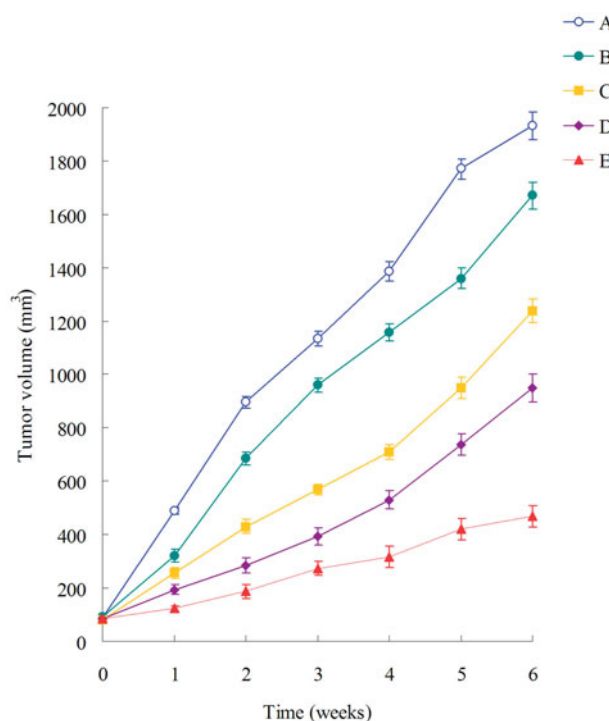

Figure 8. Effects of different formulations on tumor growth in lung cancer bearing mice. Note: (A), 0.9% sodium chloride solution; (B), free DOX; (C), DOX-DNA-NLC; (D), Pre-BN-DOX-DNA-NLC; and (E), Post-BN-DOX-DNA-NLC.

Pre-BN-DOX-DNA-NLC (51%), DOX-DNA-NLC (36%) and free DOX (13%), respectively. Figure 9 collects body weight changes of the nude mice during the test. Among all test groups, 0.9% saline and free DOX groups showed reduction in body weights. In contrast, body weights of mice in DOX-DNA-NLC and Pre-BN-DOX-DNA-NLC groups gradually increased. No noticeable body weight loss was observed in Post-BN-DOX-DNA-NLC formulation group.
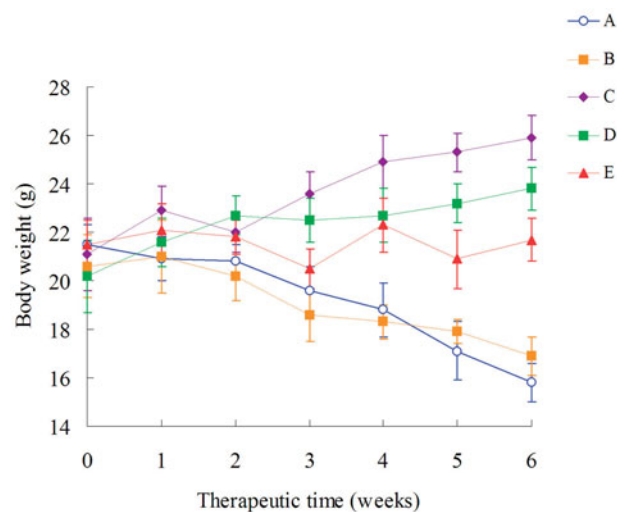

Figure 9. Body weight changes after treatment with different formulations in lung cancer bearing mice. Note: (A), 0.9% sodium chloride solution; (B), free DOX; (C), DOX-DNA-NLC; (D), Pre-BN-DOX-DNA-NLC; and (E), Post-BN-DOX-DNA-NLC.

Discussion

It is known that clinicians have been struggled the obstacles in chemotherapy for organ cancers *in vivo*: chemical anticancer drugs are lack of tumor-targeted selectivity and have severe side-effects to normal tissues (Zhao et al., 2013). In this study, a novel BN-conjugated ligand was synthesized and decorated NLC carried both DOX and DNA was investigated. We would like to see if this vector could improve the targeted ability of drugs and enhance the gene delivery effect to give a hand to the chemotherapy of lung cancer.

For the decoration in this research, two different methods were presented, post-decoration and pre-decoration, named as Post-BN-DOX-NLC and Pre-BN-DOX-NLC, respectively. For Post-BN-DOX-NLC, SA-PEG-COOH was synthesized by two-step reaction, and used to from NLC, finally BN was added to post-decorated the surface of the carriers. For Pre-BN-DOX-NLC, BN-PEG-SA was synthesized previously, and then used to construct NLC. Doxil® and Caelyx® are commercially available PEGylated nano-formulations of a conventional chemotherapeutic agent (Shahin et al., 2013). PEGylated liposomal DOX has been shown to significantly improve the therapeutic index of DOX both in preclinical and clinical studies. So we would like to use PEG as linkers for the preparation of post- and pre-decorated NLC.

Quantification experiment of conjugation of BN to NLC surface was carried out to determine the amount of modification. Table 1 summarized the particle size, zeta potential, conjugation efficiency, and conjugation ratio changed with the change of ligand to carrier ratios. As the BN ligands ratio increased, the particle size and zeta potential of Post-BN-DOX-DNA-NLC slightly increased from Post-NLC1 to Post-NLC3. While from Post-NLC3 to Post-NLC4, no obviously change was found of the size and potential. This may be the evidence that no more decoration was happened on the NLC surface. The conjugation efficiency was decreased with the increase in BN concentration over NLC. This can be explained by the steric hindrance on the nanocarriers' surface at higher ligand concentration (Accardo et al., 2012).

However the weight of BN conjugation to per mg of NLC was increased. No significant change was found between Post-NLC3 and Post-NLC4. These results demonstrated that the ligand/carrier ratio could be increased to 2 ml of BN solution versus 15 ml DOX-NLC, and then any further increase in BN ligands ratio could not bring about better decoration effect. So this ratio was determined and used for the following experiments of the post-bombesin decorated NLC. The same weight ratio of BN was calculated and applied for the post-bombesin decorated ones.

After the preparation of different formulations, physical–chemical properties including particle size, PDI, zeta potential, EE, and DL were characterized (Table 2). The size of Post-BN-DOX-DNA-NLC, Pre-BN-DOX-DNA-NLC, DOX-DNA-NLC, and blank NLC was between 130 nm and 80 nm. PDI of different formulas was from 0.096 to 0.165. Particle size can influence the properties of nanoparticles (Shariat et al., 2014). It has been reported that the solid tumor shows permeability and impaired lymphatic drainage. So nanoparticles (<200 nm) can significantly accumulate in tumor by ''filtration'' mechanism (Xu et al., 2009). Small particles are also minimal endocytosis by macrophages, so destruction and clearance could be minimized (Yu et al., 2010). A mean diameter lower than 200 nm and a PDI lower than 0.2 were considered desirable to propose the formulation for *in vitro* and *in vivo* experiments (Accardo et al., 2012). Most gene transfection and drug delivery vectors are constructed from various cationic molecules. Lipid-based schemes are composed of different cationic lipids with helper lipids such as DOTAP used in this study (Landesman et al., 2013). Cationic nanoparticles can potentially overcome such physical barriers because they penetrate into tumor tissues. Furthermore, cationic nanoparticles induce anticancer effects via electrostatic interaction between the nanoparticles and the plasma membrane (Yim et al., 2013). Cationic nanoparticles irritate the cell membrane using physical electrostatic stress irrespective to the biological resistance mechanisms (Yim & Na, 2010). All the formulations tested carried positive charges, which allowed the adsorption of vectors onto the negatively charged cell membrane through electrostatic attraction forces (He et al., 2010). Highest surface charge of Post-BN-DOX-DNA-NLC (+28.4) promoted the strongest electrostatic attraction with the cancer cells, thus delivering more drugs and genes into the targeted cells. The ability to load a sufficient amount of drug and gene is needed to achieve therapeutic efficacy (Zucker et al., 2009). The DNA·EE of Post-BN-DOX-DNA-NLC and Pre-BN-DOX-DNA-NLC were 91% and 92%, respectively. The DOX·EE of post- and pre-decorated NLC were 85% and 86%. The results demonstrated that both post- and pre-modification of BN ligands did not detach the gene and drug from the complexes and the modified vectors are stable.

In vitro accumulated DOX release profiles and DNA release profiles of were calculated. The release of DOX from Post-BN-DOX-DNA-NLC was the slowest, showing obviously sustained-release behavior over Pre-BN-DOX-DNA-NLC and DOX-DNA-NLC. The controlled delivery ability of nanocarriers for anticancer agents allows the enhancement of their therapeutic efficiency (Malzert-Fréon et al., 2006). Moreover, the use of lipid drug carriers enables sensitive

therapeutically active molecules protection against *in vivo* degradation, patient comfort increase by avoiding repetitive bolus injection or the use of perfusion pumps, as well as better drug pharmacokinetics. We hope this behavior will help with the following experiments *in vitro* and *in vivo*.

Cytotoxicity of different formulations was determined. As shown in Figure 5, significantly inhibitory effects were observed in the DOX containing formulations at the concentration of $1–20\,\mu M$, and the toxicity of all samples conformed to a dose-dependent manner. The IC_{50} values of Post-BN-DOX-DNA-NLC, Pre-BN-DOX-DNA-NLC, DOX-DNA-NLC, and free DOX were 4.5, 8.1, 12.3, and $26.7\,\mu M$, respectively. The IC_{50} of Post-BN-DOX-DNA-NLC exhibited 2-fold dose advantage over Pre-BN-DOX-DNA-NLC, 3-fold of DOX-DNA-NLC, and 6-fold compared with free DOX in reducing viability of lung cancer cells, revealing the highest tumor cell toxicity. This could be explained by the positive charge on the particle surface having high electrostatic interaction with the negatively charged tumor surface, excellent compliance of the NLC to the cell membranes, the targeting ability of BN ligands that could mediate the intracellular gene and drug delivery via both endocytic and non-endocytic pathways. 2-fold dose advantage of IC_{50} to lung cancer cells over Pre-BN-DOX-DNA-NLC showed the better performance of Post-BN-DOX-DNA-NLC.

In order to compare the gene therapy efficiency of post- and pre-decorated NLC formulations, *in vitro* and *in vivo* gene transfection studies were carried out. The *ex vivo* and *in vivo* results of NLC groups are similar, the transfection efficiency of Post-BN-DOX-DNA-NLC was significantly higher than Pre-BN-DOX-DNA-NLC ($p < 0.05$). It is worth noting that no significant differences were detected between Pre-BN-DOX-DNA-NLC and undecorated DOX-DNA-NLC *in vivo* ($p > 0.05$). This could be the evidence that post-modified gene loaded NLC have better gene delivery ability than pre-modified NLC. These results may be analyzed as follows: (1) BN played a critical role in the targeting NLC to tumor cells by receptor-mediated endocytosis. (2) Pre-decorated NLC may cover the most of BN ligands under the nanocarriers' surface and showed no better gene transfection efficiency *in vivo* due to the lack of selectivity of the carriers.

In vivo anti-tumor study was carried out on BALB/c nude mice were bearing lung cancer cells. The formulations were injection every week, and the tumor size and body weight were then monitored every week at the time before injection. The results in Figure 8 showed that Post-BN-DOX-DNA-NLC had the highest efficacy in inhibiting the tumor growth, which was about 1.5 times, 2.1 times, and 5.6 times higher than that treated with Pre-BN-DOX-DNA-NLC, DOX-DNA-NLC, and free DOX, respectively. Co-delivery of DOX and DNA into the same cells is a key for achieving synergistic effect in combined drug and gene therapy of cancer. The Post-BN-DOX-DNA-NLC have the best gene transfection ability and drug therapeutic efficacy, strongly demonstrated that DNA and DOX were co-delivered into the cancer cells by the post-decorated NLC in a better way. To sum up, the results indicates that the proposed post-BN-decorated NLC performed better than pre-BN-decorated NLC for co-delivery of anticancer drug and gene.

Conclusion

In the current study, post- and pre-BN decorated NLC were investigated to be used as a potential for drug and delivery into the tumor cells for the treatment of lung cancer. Although both decorated NLC formulations showed better transfection and anti-tumor effect than undecorated NLC and Lipofectamine *in vitro* and *in vivo*, Post-BN-DOX-DNA-NLC performed significantly better ability all the way compared to Pre-BN-DOX-DNA-NLC. The results also indicate the potent efficacy of post-BN-decorated NLC for the co-delivery of anticancer drug and gene to tumor cells. In conclusion, with the post-modification of BN, the modified co-delivery system could improve the efficacy of cancer treatment and targeted gene therapy. Post-decorated NLC systems could be used as excellent nanomedicine for the delivery of genes and/or drugs, leading to the efficiency of anti-tumor therapy.

Declaration of interest

The authors declare that they have no competing interests.

References

Abdelwahab SI, Sheikh BY, Taha MM, et al. (2013). Thymoquinone-loaded nanostructured lipid carriers: preparation, gastroprotection, in vitro toxicity, and pharmacokinetic properties after extravascular administration. Int J Nanomedicine 8:2163–72.

Accardo A, Salsano G, Morisco A, et al. (2012). Peptide-modified liposomes for selective targeting of bombesin receptors over expressed by cancer cells: a potential theranostic agent. Int J Nanomedicine 7:2007–17.

Ahn J, Miura Y, Yamada N, et al. (2015). Antibody fragment-conjugated polymeric micelles incorporating platinum drugs for targeted therapy of pancreatic cancer. Biomaterials 39:23–30.

Akhtar MJ, Ahamed M, Alhadlaq HA, et al. (2014). Targeted anticancer therapy: over expressed receptors and nanotechnology. Clin Chim Acta 436:78–92.

Armutlu P, Ozdemir ME, Uney-Yuksektepe F, et al. (2008). Classification of drug molecules considering their IC$_{50}$ values using mixed-integer linear programming based hyper-boxes method. BMC Bioinformatics 9:411.

Barve A, Jin W, Cheng K. (2014). Prostate cancer relevant antigens and enzymes for targeted drug delivery. J Control Release 187:118–32.

Carlsson N, Borde A, Wölfel S, et al. (2011). Quantification of protein concentration by the Bradford method in the presence of pharmaceutical polymers. Anal Biochem 411:116–21.

Chen Y, Yuan L, Zhou L, et al. (2012). Effect of cell-penetrating peptide-coated nanostructured lipid carriers on the oral absorption of tripterine. Int J Nanomedicine 7:4581–91.

Gandhi NS, Tekade RK, Chougule MB. (2014). Nanocarrier mediated delivery of siRNA/miRNA in combination with chemotherapeutic agents for cancer therapy: Current progress and advances. J Control Release 194C:238–56.

Hadinoto K, Sundaresan A, Cheow WS. (2013). Lipid-polymer hybrid nanoparticles as new generation therapeutic delivery platform: a review. Eur J Pharm Biopharm 85:427–43.

Han Y, Zhang Y, Li D, et al. (2014). Transferrin-modified nanostructured lipid carriers as multifunctional nanomedicine for codelivery of DNA and doxorubicin. Int J Nanomedicine 9:4107–16.

He C, Hu Y, Yin L, et al. (2010). Effects of particle size and surface charge on cellular uptake and bio distribution of polymeric nanoparticles. Biomaterials 31:3657–66.

Hejri A, Khosravi A, Gharanjig K, Hejazi M. (2013). Optimisation of the formulation of β-carotene loaded nanostructured lipid carriers prepared by solvent diffusion method. Food Chem 141:117–23.

Jiang Z, Sun C, Yin Z, et al. (2012). Comparison of two kinds of nanomedicine for targeted gene therapy: premodified or postmodified gene delivery systems. Int J Nanomedicine 7:2019–31.

Kasongo KW, Jansch M, Müller RH, Walker RB. (2011). Evaluation of the in vitro differential protein adsorption patterns of didanosine-loaded nanostructured lipid carriers (NLCs) for potential targeting to the brain. J Liposome Res 21:245–54.

Khajavinia A, Varshosaz J, Dehkordi AJ. (2012). Targeting etoposide to acute myelogenous leukaemia cells using nanostructured lipid carriers coated with transferrin. Nanotechnology 23:405101.

Kolhatkar RB, Kitchens KM, Swaan PW, Ghandehari H. (2007). Surface acetylation of polyamidoamine (PAMAM) dendrimers decreases cytotoxicity while maintaining membrane permeability. Bioconj Chem 18:2054–60.

Kolishetti N, Dhar S, Valencia PM, et al. (2010). Engineering of self-assembled nanoparticle platform for precisely controlled combination drug therapy. Proc Natl Acad Sci U S A 107:17939–44.

Kong F, Zhou F, Ge L, et al. (2012). Mannosylated liposomes for targeted gene delivery. Int J Nanomedicine 7:1079–89.

Kulhari H, Kulhari DP, Singh MK, Sistla R. (2014). Colloidal stability and physicochemical characterization of bombesin conjugated biodegradable nanoparticles. Colloids Surf A Physicochem Eng Asp 443:459–66.

Landesman-Milo D, Goldsmith M, Leviatan Ben-Arye S, et al. (2013). Hyaluronan grafted lipid-based nanoparticles as RNAi carriers for cancer cells. Cancer Lett 334:221–7.

Luan J, Yang X, Chu L, (2014). PEGylated long circulating nanostructured lipid carriers for Amoitone B: preparation, cytotoxicity and intracellular uptake. J Colloid Interface Sci 428:49–56.

Malzert-Fréon A, Vrignaud S, Saulnier P, et al. (2006). Formulation of sustained release nanoparticles loaded with a tripentone, a new anticancer agent. Int J Pharm 320:157–64.

Mosmann T. (1983). Rapid colorimetric assay for cellular growth and survival: application to proliferation and cytotoxicity assays. J Immunol Methods 65:55–63.

Nahire R, Haldar MK, Paul S, et al. (2014). Multifunctional polymersomes for cytosolic delivery of gemcitabine and doxorubicin to cancer cells. Biomaterials 35:6482–97.

Negi LM, Talegaonkar S, Jaggi M, et al. (2014). Surface engineered nanostructured lipid carriers for targeting MDR tumor: part I. Synthesis, characterization and in vitro investigation. Colloid Surf B Biointerfaces 123:600–9.

Ogawara K, Un K, Tanaka K, et al. (2009). In vivo anti-tumor effect of PEG liposomal doxorubicin (DOX) in DOX-resistant tumor-bearing mice: involvement of cytotoxic effect on vascular endothelial cells. J Control Release 133:4–10.

Peeters L, Sanders NN, Jones A, et al. (2007). Post-PEGylated lipoplexes are promising vehicles for gene delivery in RPE cells. J Control Release 121:208–17.

Shahin M, Soudy R, El-Sikhry H, et al. (2013). Engineered peptides for the development of actively tumor targeted liposomal carriers of doxorubicin. Cancer Lett 334:284–92.

Shao Z, Shao J, Tan B, et al. (2015). Targeted lung cancer therapy: preparation and optimization of transferrin-decorated nanostructured lipid carriers as novel nanomedicine for co-delivery of anticancer drugs and DNA. Int J Nanomedicine 10:1223–33.

Shariat S, Badiee A, Jalali SA, et al. (2014). P5 HER2/neu-derived peptide conjugated to liposomes containing MPL adjuvant as an effective prophylactic vaccine formulation for breast cancer. Cancer Lett 355:54–60.

Shi F, Yang G, Ren J, et al. (2013). Formulation design, preparation, and in vitro and in vivo characterizations of β-Elemene-loaded nanostructured lipid carriers. Int J Nanomedicine 8:2533–41.

Taratula O, Kuzmov A, Shah M, et al. (2013). Nanostructured lipid carriers as multifunctional nanomedicine platform for pulmonary co-delivery of anticancer drugs and siRNA. J Control Release 171:349–57.

Tsouris V, Joo MK, Kim SH, et al. (2014). Nano carriers that enable co-delivery of chemotherapy and RNAi agents for treatment of drug-resistant cancers. Biotechnol Adv 32:1037–50.

Wang W, Xi M, Duan X, et al. (2015). Delivery of baicalein and paclitaxel using self-assembled nanoparticles: synergistic antitumor effect in vitro and in vivo. Int J Nanomedicine 10:3737–50.

Wicki A, Witzigmann D, Balasubramanian V, Huwyler J. (2015). Nanomedicine in cancer therapy: challenges, opportunities, and clinical applications. J Control Release 200:138–57.

Xu Z, Chen L, Gu W, et al. (2009). The performance of docetaxel-loaded solid lipid nanoparticles targeted to hepatocellular carcinoma. Biomaterials 30:226–32.

Yang F, Hu J, Yang D, et al. (2009). Pilot study of targeting magnetic carbon nanotubes to lymph nodes. Nanomedicine (Lond) 4:317–30.

Yang F, Jin C, Jiang Y, et al. (2011). Liposome based delivery systems in pancreatic cancer treatment: from bench to bedside. Cancer Treat Rev 37:633–42.

Yang XY, Li YX, Li M, et al. (2013). Hyaluronic acid-coated nanostructured lipid carriers for targeting paclitaxel to cancer. Cancer Lett 334:338–45.

Yim H, Na K. (2010). Polycationic nanodrug covered with hyaluronic acid for treatment of P-glycoprotein over expressing cancer cells. Biomacromolecules 11:2387–93.

Yim H, Park SJ, Bae YH, Na K. (2013). Biodegradable cationic nanoparticles loaded with an anticancer drug for deep penetration of heterogeneous tumours. Biomaterials 34: 7674–82.

Yu W, Liu C, Liu Y, et al. (2010). Mannan-modified solid lipid nanoparticles for targeted gene delivery to alveolar macrophages. Pharm Res 27:1584–96.

Yu W, Zhang N. (2009). Surface modifcation of nanocarriers for cancer therapy. Curr Nanosci 5:123–34.

Zhang XG, Miao J, Dai YQ, et al. (2008). Reversal activity of nanostructured lipid carriers loading cytotoxic drug in multi-drug resistant cancer cells. Int J Pharm 361:239–44.

Zhao YZ, Dai DD, Lu CT, et al. (2013). Epirubicin loaded with propylene glycol liposomes significantly overcomes multidrug resistance in breast cancer. Cancer Lett 330:74–83.

Zucker D, Marcus D, Barenholz Y, Goldblum A. (2009). Liposome drugs' loading efficiency: a working model based on loading conditions and drug's physicochemical properties. J Control Release 139:73–80.